

# Mechanisms of enhanced orbital dia- and paramagnetism: Application to the Rashba semiconductor BiTeI

G. A. H. Schober,<sup>1,2,3,\*</sup> H. Murakawa,<sup>4</sup> M. S. Bahramy,<sup>4</sup>  
R. Arita,<sup>1,4</sup> Y. Kaneko,<sup>5</sup> Y. Tokura,<sup>1,3,4,5</sup> and N. Nagaosa<sup>1,3,4,†</sup>

<sup>1</sup>*Department of Applied Physics, University of Tokyo, Tokyo 113-8656, Japan*

<sup>2</sup>*Institute for Theoretical Physics, University of Heidelberg, D-69120 Heidelberg, Germany*

<sup>3</sup>*Cross-Correlated Materials Research Group (CMRG), ASI, RIKEN, Wako 351-0198, Japan*

<sup>4</sup>*Correlated Electron Research Group (CERG), ASI, RIKEN, Wako 351-0198, Japan*

<sup>5</sup>*Multiferroics Project, Exploratory Research for Advanced Technology (ERATO),*

*Japan Science and Technology Agency (JST), c/o Department of Applied Physics, University of Tokyo, Tokyo 113-8656, Japan*

(Dated: December 3, 2024)

We study the magnetic susceptibility of a layered semiconductor BiTeI with giant Rashba spin splitting both theoretically and experimentally to explore its orbital magnetism. Apart from the core contributions, a large temperature-dependent diamagnetic susceptibility is observed when the Fermi energy  $E_F$  is near the crossing point of the conduction bands, while the susceptibility turns to be paramagnetic when  $E_F$  is away from it. These features are consistent with first-principles calculations, which also predict an enhanced orbital magnetic susceptibility with both positive and negative signs as a function of  $E_F$  due to band (anti)crossings. Based on these observations, we propose two mechanisms for an enhanced paramagnetic orbital susceptibility.

PACS numbers: 75.20.Ck, 71.70.Ej, 85.75.-d, 31.15.A-, 71.15.-m

The magnetic susceptibility  $\chi$  is one of the most fundamental physical quantities, revealing invaluable information about the spin and orbital states of solid materials [1]. The sign of  $\chi$ , depending sensitively on the mechanism of the magnetization, plays a crucial role in identifying the magnetic properties of bulk systems. From this viewpoint, solid materials are roughly classified into the following three categories [1]: (i) band insulators with weak temperature-independent diamagnetism  $\chi < 0$ , (ii) metals with temperature-independent Pauli paramagnetic susceptibility  $\chi_P > 0$  and temperature-independent Landau diamagnetic susceptibility  $\chi_L < 0$  well below the Fermi temperature  $T \ll T_F = E_F/k_B$ , and (iii) magnetic materials with local moments with strongly temperature-dependent Curie paramagnetic susceptibility  $\chi(T) \propto 1/T$  or Curie-Weiss law  $\chi(T) \propto 1/(T - T_0)$  corresponding to ferromagnetic ( $T_0 > 0$ ) or antiferromagnetic ( $T_0 < 0$ ) interactions between the magnetic moments. When an electron configuration with  $J = 0$  ( $J$ : total angular momentum) is realized for a magnetic ion, e.g., in the case of four  $d$ -electrons, Larmor diamagnetism and van-Vleck paramagnetism compete to determine the sign of  $\chi$ .

Usually, the orbital motion of electrons leads to a diamagnetic  $\chi$ , as in the case of Larmor and Landau diamagnetism. This is due to the cyclotron motion induced by the Lorentz force, which tends to reduce the action of the external magnetic field. When the band gap is reduced or fully closed, this diamagnetic susceptibility is considerably enhanced as in the cases of bismuth [2] and graphene [3]. Especially in graphene, due to the presence of gapless two-dimensional Dirac fermions,  $\chi$  diverges as  $\propto -1/T$  as  $T \rightarrow 0$  [3]. Despite this general tendency, there is no proof that the orbital motion always favors

diamagnetism, in particular in the presence of strong spin-orbit interaction (SOI). Hence one cannot exclude the possibility that orbital paramagnetism may be realized in band insulators and metals. As a matter of fact, Kubo and Obata [4] have shown that for metals with partially filled degenerate bands, the orbital paramagnetic susceptibility can be of the same order of magnitude as the Pauli spin susceptibility. For band insulators, however, it has so far been an open question whether orbital paramagnetism can be realized or not.

In this paper, we address this question by studying the orbital magnetism in BiTeI, a narrow-gap polar semiconductor with a noncentrosymmetric layered structure. Due to the polarity of the bulk material and the presence of Bi atoms with large atomic SOI, BiTeI exhibits an extraordinarily large bulk Rashba spin splitting (RSS), astonishingly reaching  $\simeq 400$  meV at the bottom of the conduction band as observed in the recent angle-resolved photoemission spectroscopy experiment by Ishizaka *et al.* [5]. Further studies based on optical spectroscopy [6], first-principles calculations and group theoretical analysis [7] have confirmed that this giant RSS is indeed a bulk property of BiTeI, and revealed that in addition to the bottom conduction bands (BCB's), the top valence bands (TVB's) of BiTeI are subject to a comparable RSS. These unique features make BiTeI an ideal medium to explore different aspects of orbital magnetism in a band insulating system. Below we theoretically predict and experimentally confirm that in BiTeI, both an enhanced orbital diamagnetism and an unconventional orbital paramagnetism can be realized by tuning the Fermi energy  $E_F$ . This intriguing behavior is shown to be a direct consequence of the RSS.

As described in Refs. 5 and 7, BiTeI has a minimum band gap not at the Brillouin zone (BZ) center, but around the hexagonal face center of the BZ, referred to as point *A*, as shown in Fig. 1(a). Due to the strong covalency and ionicity of Bi-Te and Bi-I bonds, respectively, the BCB's are dominated by Bi-6*p* states, whereas the TVB's are predominantly of Te-5*p* character with a partial contribution from I-5*p* states. The huge SOI of Bi accompanied by a strong negative crystal field splitting of TVB's leads BCB's and TVB's to be symmetrically of the same character, and hence to be strongly coupled with each other via a quasi-two-dimensional RSS Hamiltonian. Near point *A*, this can be described as [7]

$$H_R = \frac{\mathbf{p}^2}{2m^*} + \lambda \mathbf{e}_z \cdot (\mathbf{s} \times \mathbf{p}), \quad (1)$$

where  $m^*$  is the effective mass of the carriers,  $\lambda$  is the Rashba parameter,  $\mathbf{e}_z$  is the unit vector in  $z$  direction, which is the direction of the potential gradient breaking the inversion symmetry, and  $\mathbf{s}$  and  $\mathbf{p}$  are the spin and momentum operators, respectively. As fitting parameters,  $m^*$  and  $\lambda$  can be tuned [8] such that  $H_R$  can properly reproduce the electronic dispersion of BCB's around point *A*, in particular the momentum offset of the conduction band minimum (CBM),  $|\mathbf{p}| = \hbar k_0$  with  $k_0 = 0.052 \text{ \AA}^{-1}$ , and the Rashba energy  $E_R = 113 \text{ meV}$ , where  $E_R$  is the energy of the conduction bands at their crossing point with respect to CBM.

The above two-dimensional (2D) Rashba model can be exactly solved under a perpendicular magnetic field  $\mathbf{B}$  [9] to obtain the free energy density  $F$  and the orbital (volume) magnetic susceptibility  $\chi_v = -\mu_0 \partial^2 F / \partial B^2$ , where  $\mu_0$  is the vacuum permeability. We have defined the molar susceptibility as  $\chi = A_{\text{mol}} \chi_v$ , where  $A_{\text{mol}} = 9.8 \text{ cm}^2/\text{mol}$  is the molar surface area of one BiTeI layer. Fig. 1(b) shows the calculated dependence of  $\chi$  on the Fermi energy  $E_F$ . Near the band crossing point, where we take the origin of  $E_F$ , an enhanced diamagnetic susceptibility is observed, which diverges as  $\chi \propto -1/T$  as in the case of graphene [3]. For  $E_F \gg E_R$ ,  $\chi$  approaches  $-A_{\text{mol}} \mu_0 e^2 / (12\pi m^*)$ , which is equivalent to the value of the Landau diamagnetic susceptibility for free electrons with mass  $m^*$  in 2D, normalized by  $A_{\text{mol}}$ . In addition, we find a paramagnetic orbital susceptibility when  $E_F$  is below the band crossing point, which is a unique feature attributed to the Rashba spin splitting. A simple explanation for this paramagnetic behavior can be given as follows: Let us define  $\eta^2 = 2E_R / \hbar \omega_0$ , where  $E_R$  is the Rashba energy in the absence of the magnetic field, and  $\omega_0 = eB / m^*$  is the cyclotron frequency. Assuming that  $\eta^2 > 1$ , it turns out that there is always a natural number  $N$  such that  $|2N - \eta^2| < 1$ . It follows that at least one Landau level,  $E_{N-}$ , is lower in energy than the bottom of the Rashba-split bands,

$$E_{N-} = \hbar \omega_0 (N - \frac{1}{2} \sqrt{1 + 8N\eta^2}) < -E_R \quad (2)$$

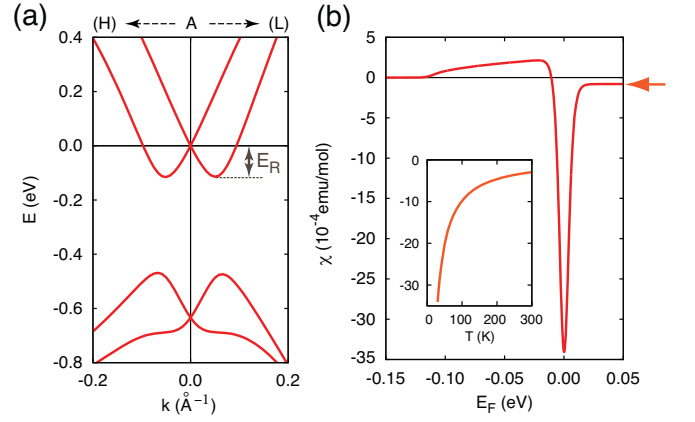


FIG. 1. (Color online) (a) Band dispersion of BiTeI near point *A* towards the *H* and *L* directions. The crossing point of the conduction bands is set at zero energy. (b) Orbital magnetic susceptibility obtained from a 2D Rashba model, which reproduces the dispersion of the BCB's in BiTeI around point *A*. The main panel shows the Fermi energy dependence of  $\chi$  at  $T = 30 \text{ K}$ . The arrow marks the value of the Landau diamagnetic susceptibility for free electrons with mass  $m^*$  in 2D (see the related discussion). The inset shows the temperature dependence of the diamagnetic peak value at  $E_F = 0$ , diverging as  $-1/T$ .

Accordingly, for sufficiently low filling of these bands, by applying  $\mathbf{B}$  the total energy of the system is lowered, a sign for the occurrence of paramagnetism. Since the Landau-Peierls formula [10], which takes into account only intraband contributions, gives a negative value for the orbital magnetic susceptibility, this positive  $\chi$  can be attributed to the interband contributions, which are allowed due to the RSS of BCB's. Also note that this behavior is different from that in the 2D Dirac model describing graphene, which shows only a diamagnetic orbital susceptibility.

To corroborate these results as well as to explore the effects of all energy bands, we have performed a detailed analysis based on first-principles density functional theory (DFT). The orbital (molar) magnetic susceptibility of BiTeI has been computed using the Fukuyama formula [11],

$$\chi(T) = \mu_0 \frac{N_A}{N} \frac{e^2 \hbar^2}{2} k_B T \sum_{\ell} \sum_{\mathbf{k}} \text{Tr} [G v_x G v_y G v_x G v_y], \quad (3)$$

where  $N_A$  is the Avogadro constant,  $N$  the number of carriers,  $G = [i\omega_{\ell} + E_F - H]^{-1}$  the one-particle thermal Green's function with Matsubara frequency  $\omega_{\ell} = (2\ell + 1)\pi k_B T$ , and  $v_i$  ( $i = x, y, z$ ) the velocity operator represented in matrix form as

$$v_{i,nm} = \langle n | v_i(\mathbf{k}) | m \rangle = \frac{1}{\hbar} \left\langle n \left| \frac{\partial H(\mathbf{k})}{\partial k_i} \right| m \right\rangle, \quad (4)$$

where  $|n\rangle$  corresponds to the  $n$ th eigenstate of  $H(\mathbf{k})$ .

The numerical computation of  $v_{i,nm}$  has been done using the approach of Ref. 12, whereby  $H(\mathbf{k})$  is described in the basis of so-called maximally localized Wannier functions (MLWF's) [13]. To fully take into account the contributions of all possible energy states, a set of 18 MLWF's, spanning the 12 highest valence bands and 6 lowest conduction bands, has been generated with the WANNIER90 code [14] by postprocessing [15] the first-principles relativistic DFT calculations, initially done using the WIEN2K package [16] (see Ref. 7 for details). We have also calculated the Pauli paramagnetic susceptibility  $\chi_P$ , leaving the orbital degree of freedom unaffected. Namely we have added only the Zeeman coupling  $-\mu_B \boldsymbol{\sigma} \cdot \mathbf{B}$  to the Hamiltonian and calculated the spin magnetization to obtain  $\chi_P$ . However, the contribution of  $\chi_P$  is much smaller than the orbital  $\chi$  as described below.

Fig. 2 shows the  $E_F$  dependence of  $\chi + \chi_P$  obtained by the first-principles calculations for BiTeI taking into account the dispersion along  $k_z$  direction, where the origin of  $E_F$  is taken at the crossing point of BCB's at point A. The Pauli contribution is an order of magnitude smaller than the orbital  $\chi$ , at least in the considered range of  $-0.15 \text{ eV} \leq E_F \leq 0.15 \text{ eV}$ . This is due to the small effective mass of BCB carriers within the hexagonal face of the BZ (hereafter referred to as  $ab$  plane),  $m^* \simeq 0.2m$  [6]. This is analogous to the case of bismuth [2] and can be understood by considering a spin-degenerate two-dimensional parabolic band  $E = \hbar^2 k^2 / (2m^*)$ . Then the orbital and Pauli susceptibility are given by  $\chi = -(1/3)\mu_0 N_A \mu_B^{*2} / E_F$  and  $\chi_P = \mu_0 N_A \mu_B^2 / E_F$ , respectively, where  $\mu_B^* = e\hbar / (2m^*)$ ,  $\mu_B = e\hbar / (2m)$ , and  $E_F = \hbar^2 k_F^2 / (2m^*)$  with the Fermi wave vector  $k_F$ . Since  $m^*$  appears in  $E_F$ , but not in the spin-interaction term, i.e. in  $\mu_B$ , it turns out that  $\chi_P = -3(m^*/m)^2 \chi \simeq -0.1\chi$ . Therefore we can neglect  $\chi_P$  and focus on  $\chi$  below.

For  $\mathbf{B}$  parallel to  $\mathbf{e}_z$ , near the band crossing point a large temperature-dependent diamagnetic susceptibility is observed, while the susceptibility turns to be paramagnetic and temperature-independent when  $E_F$  is away from it. In contrast, if  $\mathbf{B}$  is applied perpendicular to the  $z$  direction,  $\chi$  is found to be always positive and almost insensitive to  $E_F$ . The calculated results are in good agreement with the experiment, as shown in Fig. 2.

For the experimental measurement of  $\chi$ , single crystals of BiTeI with various charge carrier densities were grown by a Bridgman method or chemical vapor transport. The obtained crystals have cleaved (001) planes. The charge carrier density of each sample was determined by the Hall resistivity measurement. The magnetization measurement was performed with use of the vibrating-sample magnetometer. The sample holder for this was made of a plastic straw tube, whose tiny diamagnetic signal was accurately subtracted.

To extract the orbital magnetic susceptibility from the experimental data, one needs to subtract the Larmor sus-

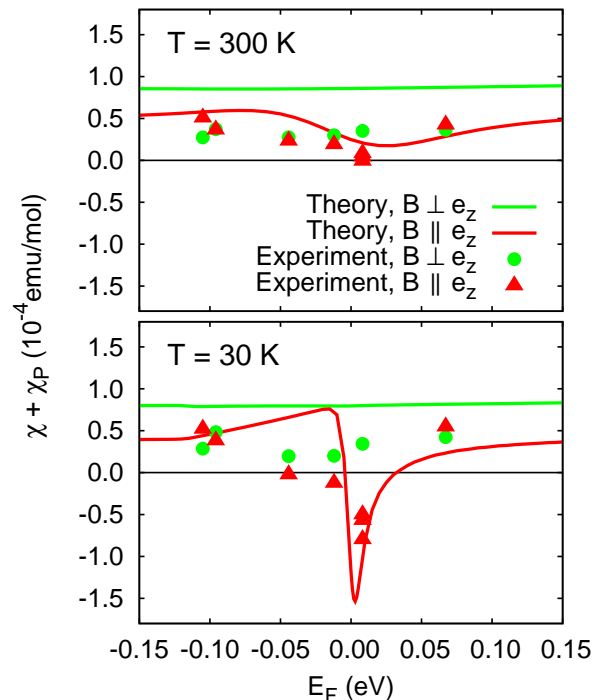


FIG. 2. (Color online) Magnetic susceptibility of BiTeI as a function of Fermi energy  $E_F$ , at two temperatures  $T = 300 \text{ K}$  (upper panel) and  $T = 30 \text{ K}$  (lower panel). Solid lines represent the calculated susceptibility including the Pauli contribution, and points show the corresponding experimental data after subtracting the core contributions.  $E_F = 0$  corresponds to the crossing point of the Rashba-split conduction bands at point A.

ceptibly  $\chi_L$  originating from the individual ionic cores in BiTeI. Since in this material the ionic states of Bi, Te and I ions are  $3+$ ,  $2-$  and  $1-$ , respectively, one can assume that they all have closed shell ionic configurations. Accordingly, for each ion  $\chi_L$  can be easily estimated as [1],  $\chi_L = -\mu_0 N_A (e^2 / 6m) \sum_{i=n,l,j} Z_i \langle r^2 \rangle_i$ , where  $Z_i$  is the number of electrons occupying state  $i = \{n, l, j\}$ . Performing a set of all-electron DFT calculations using the LDA1.X program [17], the spread functions  $\langle r^2 \rangle_i$  have been individually calculated for all the occupied states of  $\text{Bi}^{3+}$ ,  $\text{Te}^{2-}$  and  $\text{I}^{1-}$  (see Table 1 in the supplemental material). Based on these calculations, the respective  $\chi_L$  of  $\text{Bi}^{3+}$ ,  $\text{Te}^{2-}$  and  $\text{I}^{1-}$  are found to be  $-32.5$ ,  $-23.3$  and  $-21.1$  (all in units of  $10^{-6} \text{ emu/mol}$ ). We have accordingly subtracted these values from our experimental data to deduce the orbital magnetic susceptibility.

In Fig. 3, we show the temperature dependence of the orbital magnetic susceptibility for  $\mathbf{B} \parallel \mathbf{e}_z$  at two characteristic Fermi energies, one near the band crossing point and the other away from it. In the first case, a strong temperature dependence and sign change of  $\chi$  from paramagnetism to diamagnetism is observed as the temper-

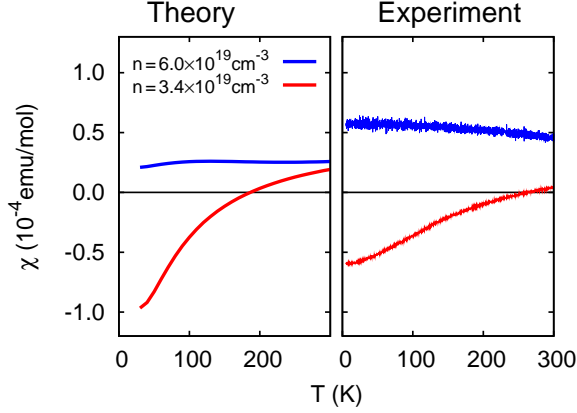


FIG. 3. (Color online) Temperature dependence of the orbital magnetic susceptibility of BiTeI for  $\mathbf{B} \parallel \mathbf{e}_z$ , obtained theoretically (left panel) and experimentally (right panel) at two characteristic carrier densities. For  $n = 3.4 \times 10^{19} \text{cm}^{-3}$  the Fermi energy  $E_F$  is close to the band crossing point, whereas for  $n = 6.0 \times 10^{19} \text{cm}^{-3}$  it is  $\simeq 70 \text{ meV}$  above it.

ature is lowered, while in the latter case the susceptibility remains paramagnetic and almost independent of temperature. This behavior is clearly understood in terms of the temperature-dependent enhanced diamagnetic contribution near  $E_F = 0$ , which adds to the almost temperature-independent paramagnetic interband contribution. All these features are in excellent agreement with the experimental curves measured at two different samples with corresponding carrier densities, as shown in Fig 3.

Up to now, we have focused on the experimentally accessible region  $-0.15 \text{ eV} < E_F < 0.15 \text{ eV}$ . It is of interest to study  $\chi$  in an extended region to reveal the mechanism of the enhanced orbital magnetism. Fig. 4(a) shows the calculated orbital magnetic susceptibility as a function of  $E_F$  over the whole energy range of the 18-band model at  $T = 300 \text{ K}$ . Large positive and negative values are observed, which can be attributed to (anti)crossings in the band structure of BiTeI. As shown in Fig. 4(b), these are further even enhanced if we consider only the contribution from the  $ab$  plane of the BZ. Indeed, a careful comparison between Fig. 4(b) and Fig. 2(d) of Ref. 7 reveals that for energies with major paramagnetic/diamagnetic peaks, the corresponding energy states in the  $ab$  plane undergo several band crossings or anticrossings thereby forming a number of Dirac-like cones, mainly with tilted shapes [for example in Fig. 2(d) of Ref. 7, see the valence bands along  $A - L - H - A$  direction within the energy window from  $-4 \text{ eV}$  to  $-2 \text{ eV}$ ]. By this analysis it accordingly turns out that the quasi-two-dimensionality plays an important role in enhancing the diamagnetic and paramagnetic orbital susceptibility due to the band

(anti)crossings.

To clarify this point, we provide a model to explain the divergent paramagnetic orbital susceptibility near the band crossings as the temperature  $T \rightarrow 0$ . Our model describes a tilted 2D Dirac cone,

$$H = v\mathbf{k} \cdot \boldsymbol{\sigma} + \mathbf{v}' \cdot \mathbf{k}, \quad (5)$$

where the two bands cross at  $\mathbf{k} = \mathbf{0}$ , and the Fermi energy is at  $E = 0$ .  $\boldsymbol{\sigma}$  is the vector of Pauli matrices describing the two bands. The energy dispersion is given by  $\varepsilon_{\pm}(\mathbf{k}) = \mathbf{v}' \cdot \mathbf{k} \pm v|\mathbf{k}|$ , and hence the Fermi surface differs dramatically between the two cases: (a)  $v > v' = |\mathbf{v}'|$  and (b)  $v < v' = |\mathbf{v}'|$ . In case (a), the Fermi surface is a point, while it is given by two lines  $k_y = \pm \sqrt{v'^2 - v^2} k_x / v$  in case (b). (Here we assume that  $\mathbf{v}' \parallel \mathbf{e}_x$ .) The contribution from the band crossing region to the orbital magnetic susceptibility  $\chi$  can be estimated by using Eq. (3) applied to the  $2 \times 2$  Green's function. This reveals the asymptotic behavior of  $\chi$  in the low temperature limit as:  $\chi \propto -1/T$  in case (a), while  $\chi \propto 1/T$  in case (b). Therefore, in contrast to the naive expectation that the orbital motion leads to diamagnetism, the tilted band crossing

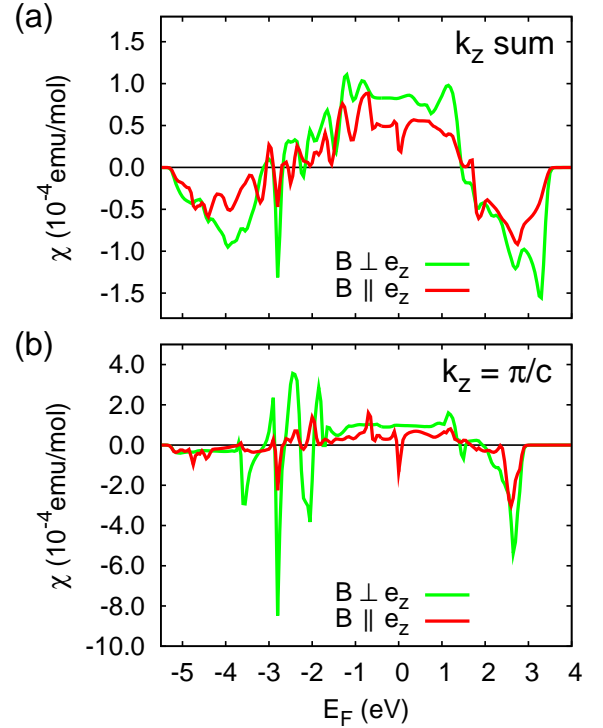


FIG. 4. (Color online) Theoretical results for the orbital magnetic susceptibility in the entire energy range of the 18-band model of BiTeI at  $T = 300 \text{ K}$ . For (a) we have performed in Eq. (3) the  $\mathbf{k}$  integral over the whole three-dimensional Brillouin zone, whereas for (b) we have calculated only the contribution from the  $ab$  plane, i.e., we have assumed the integrand to be independent of  $k_z$  and taken only the value at  $k_z = \pi/c$ .

with  $v < v'$  leads to diverging orbital paramagnetism in two dimensions.

In summary, we have studied the orbital magnetism focusing on its enhancement due to interband effects. As a concrete example we have considered BiTeI with its giant Rashba splitting to see how the spin-orbit interaction affects the orbital magnetism. In addition to the temperature-dependent large diamagnetic susceptibility near the band crossing point analogous to graphene, we have found two mechanisms for the enhanced orbital *paramagnetism*. One is the Rashba splitting with the Fermi energy below the band crossing, and the other is the tilted band crossing.

This research is supported by MEXT Grand-in-Aid No. 20740167, 19048008, 19048015, and 21244053, Strategic International Cooperative Program (Joint Research Type) from Japan Science and Technology Agency, and by the Japan Society for the Promotion of Science (JSPS) through its “Funding Program for World-Leading Innovative R & D on Science and Technology (FIRST Program)”. G. A. H. S. acknowledges support from MEXT and DAAD.

---

\* g.schober@thphys.uni-heidelberg.de

† nagaosa@ap.t.u-tokyo.ac.jp

- [1] N. W. Ashcroft and N. D. Mermin, *Solid State Physics* (W.B. Saunders Company, 1976).
- [2] W. Nolting and A. Ramakanth, *Quantum Theory of Magnetism* (Springer, 2009); H. Fukuyama and R. Kubo, J. Phys. Soc. Jpn. **28**, 570 (1970).
- [3] A. H. Castro Neto, F. Guinea, N. M. R. Peres, K. S. Novoselov, and A. K. Geim, Rev. Mod. Phys. **81**, 109 (2009).
- [4] R. Kubo and Y. Obata, J. Phys. Soc. Jpn. **11**, 547 (1956).
- [5] K. Ishizaka *et al.*, Nature Mater. **10**, 521 (2011).
- [6] J. S. Lee *et al.*, Phys. Rev. Lett. **107**, 117401 (2011).
- [7] M. S. Bahramy, R. Arita, and N. Nagaosa, Phys. Rev. B **84**, 041202(R) (2011).
- [8] In our 2D model,  $m^*$  and  $\lambda$  are set to 0.09 $m$  ( $m$ : electron mass) and 4.3 eVÅ, respectively.
- [9] S.-Q. Shen, M. Ma, X. C. Xie, and F. C. Zhang, Phys. Rev. Lett. **92**, 256603 (2004).
- [10] L. D. Landau, Z. Phys. **64**, 629 (1930); R. Peierls, Z. Phys. **80**, 763 (1933).
- [11] H. Fukuyama, Prog. Theor. Phys. **45**, 704 (1971).
- [12] X. Wang, J. R. Yates, I. Souza, and D. Vanderbilt, Phys. Rev. B **74**, 195118 (2006).
- [13] N. Marzari and D. Vanderbilt, Phys. Rev. B **56**, 12847 (1997); I. Souza, N. Marzari, and D. Vanderbilt, Phys. Rev. B **65**, 035109 (2001).
- [14] A. A. Mostofi *et al.*, Comput. Phys. Commun. **178**, 685 (2008).
- [15] J. Kunes *et al.*, Comput. Phys. Commun. **181**, 1888 (2010).
- [16] P. Blaha *et al.*, WIEN2K package: <http://www.wien2k.at>.
- [17] LDA1.X is a utility code implemented in the program package QANTUMESPRESSO, which is freely available at: <http://www.quantum-espresso.org/>.

Supplementary information for  
**Mechanisms of enhanced orbital dia- and paramagnetism:  
Application to the Rashba semiconductor BiTeI**

G. A. H. Schober,<sup>1,2,3,\*</sup> H. Murakawa,<sup>4</sup> M. S. Bahramy,<sup>4</sup>  
R. Arita,<sup>1,4</sup> Y. Kaneko,<sup>5</sup> Y. Tokura,<sup>1,3,4,5</sup> and N. Nagaosa<sup>1,3,4,†</sup>

<sup>1</sup>*Department of Applied Physics, University of Tokyo, Tokyo 113-8656, Japan*

<sup>2</sup>*Institute for Theoretical Physics, University of Heidelberg, D-69120 Heidelberg, Germany*

<sup>3</sup>*Cross-Correlated Materials Research Group (CMRG),  
ASI, RIKEN, Wako 351-0198, Japan*

<sup>4</sup>*Correlated Electron Research Group (CERG),  
ASI, RIKEN, Wako 351-0198, Japan*

<sup>5</sup>*Multiferroics Project, Exploratory Research for Advanced Technology (ERATO),  
Japan Science and Technology Agency (JST),  
c/o Department of Applied Physics,  
University of Tokyo, Tokyo 113-8656, Japan*

---

\* g.schober@thphys.uni-heidelberg.de

† nagaosa@ap.t.u-tokyo.ac.jp

TABLE I.

Estimated  $\langle r^2 \rangle$  values for core and valence states of  $\text{Bi}^{3+}$ ,  $\text{Te}^{2-}$  and  $\text{I}^-$ . Values are in  $\text{\AA}^2$ .

state	$\text{Bi}^{3+}$	$\text{Te}^{2-}$	$\text{I}^-$
1s	0.0000	0.0003	0.0003
2s	0.0015	0.0047	0.0045
2p( $j = 1/2$ )	0.0010	0.0035	0.0033
2p( $j = 3/2$ )	0.0015	0.0037	0.0037
3s	0.0094	0.0332	0.0316
3p( $j = 1/2$ )	0.0085	0.0317	0.0301
3p( $j = 3/2$ )	0.0103	0.0340	0.0323
4s	0.0449	0.1851	0.1732
3d( $j = 3/2$ )	0.0078	0.0288	0.0272
3d( $j = 5/2$ )	0.0083	0.0295	0.0279
4p( $j = 1/2$ )	0.0455	0.2053	0.1906
4p( $j = 3/2$ )	0.0541	0.2202	0.2048
4d( $j = 3/2$ )	0.0560	0.3070	0.2748
4d( $j = 5/2$ )	0.0589	0.3150	0.2818
5s	0.2169	1.4443	1.2830
5p( $j = 1/2$ )	0.2472	2.6374	2.2199
5p( $j = 3/2$ )	0.2995	3.1136	2.6245
4f( $j = 5/2$ )	0.0642		
4f( $j = 5/2$ )	0.0659		
5d( $j = 3/2$ )	0.4610		
5d( $j = 5/2$ )	0.4923		
6s	1.2707		